LIBRARY
RESEARCH REPORTS DIVISION
NAVAL POSTGRADUATE SCHOOL
MONTEREY, CALIFORNIA 93940

NPS63-82-002

NAVAL POSTGRADUATE SCHOOL

Monterey, California

MIXED LAYER MODELING OF AEROSOLS
IN THE MARINE BOUNDARY LAYER

by

K. L. Davidson, C. W. Fairall,
and G. E. Schacher

May 1982

Technical Report

Approved for public release; distribution unlimited.

Prepared for: Naval Ocean Systems Center
San Diego, California 92152

FEDDOCS
D 208.14/2:
NPS-63-82-002

DUDLEY KNOX LIBRARY
NAVAL POSTGRADUATE SCHOOL
MONTEREY, CA 93943-5101

NAVAL POSTGRADUATE SCHOOL
Monterey, California

Rear Admiral J. J. Ekelund
Superintendent

David A. Schrady
Acting Provost

The work reported herein was supported in part by the Naval Ocean Systems Center, San Diego, California.

Reproduction of all or part of this report is authorized.

This report was prepared by:

DUDLEY KNOX LIBRARY
NAVAL POSTGRADUATE SCHOOL
MONTEREY, CA 93943-5101

Unclassified

SECURITY CLASSIFICATION OF THIS PAGE (When Data Entered)

REPORT DOCUMENTATION PAGE

READ INSTRUCTIONS BEFORE COMPLETING FORM

1. REPORT NUMBER: NPS63-82-002
2. GOVT ACCESSION NO.:
3. RECIPIENT'S CATALOG NUMBER:

4. TITLE (and Subtitle): Mixed Layer Modeling of Aerosols in the Marine Boundary Layer
5. TYPE OF REPORT & PERIOD COVERED: Technical Report
6. PERFORMING ORG. REPORT NUMBER:

7. AUTHOR(s): K. L. Davidson, C. W. Fairall* and G. E. Schacher
8. CONTRACT OR GRANT NUMBER(s):

9. PERFORMING ORGANIZATION NAME AND ADDRESS: Naval Postgraduate School, Monterey, California 93940
10. PROGRAM ELEMENT, PROJECT, TASK AREA & WORK UNIT NUMBERS: 62759N:SF59551697 N6600182WR00017

11. CONTROLLING OFFICE NAME AND ADDRESS: Naval Ocean Systems Center, San Diego, California 92152
12. REPORT DATE: March 1982
13. NUMBER OF PAGES: 51

14. MONITORING AGENCY NAME & ADDRESS (if different from Controlling Office):
15. SECURITY CLASS. (of this report): Unclassified
15a. DECLASSIFICATION/DOWNGRADING SCHEDULE:

16. DISTRIBUTION STATEMENT (of this Report): Approved for public release; distribution unlimited.

17. DISTRIBUTION STATEMENT (of the abstract entered in Block 20, if different from Report):

18. SUPPLEMENTARY NOTES: *BDM Corp., Contract Employee

19. KEY WORDS (Continue on reverse side if necessary and identify by block number): Marine Aerosols, Boundary Layer Modeling

20. ABSTRACT (Continue on reverse side if necessary and identify by block number)

A mixed layer dynamic model for the structure and evolution of aerosols in the marine regime is presented. The ambient aerosol spectrum is divided [illegible] the continental and sea salt components and transformed to a reference saturation ratio, S = 0.8 (80% relative humidity). The temporal evolution of the aerosol spectrum is predicted from rate equations which require a specification of the surface production rate, the entrainment rate (W_e) and the mixed layer depth (h). The model was tested against a marine data set obtained [illegible]

DD FORM 1 JAN 73 1473 EDITION OF 1 NOV 65 IS OBSOLETE S/N 0102-014-6601

Unclassified

SECURITY CLASSIFICATION OF THIS PAGE (When Data Entered)

Southern California during the CEWCOM-78 experiment. The test was with two different methods of obtaining the relevant meteorological and aerosol parameters: 1) actual measurements and 2) dynamic boundary layer model prediction and parameterization. In the first case the model reproduced the aerosol data within a factor of 1.5 while in the second case the uncertainty factor was 2.0. In either case the model only modestly outperforms the much simpler Wells-Munn-Katz (WMK) model, which uses only local specification of the wind speed and humidity. Suggested improvements of the mixed layer model are presented.

TABLE OF CONTENTS

1. Introduction - 7

2. Description and Evaluation of Existing Aerosol Models - - - - 9

3. Boundary Layer Model - 14

4. Aerosol Considerations in a Well Mixed Layer - - - - - - - - - 18

5. Marine Boundary Layer Experiment - - - - - - - - - - - - - - - 22

6. Aerosol Model Test - 30

   a. Aerosol Surface Flux - - - - - - - - - - - - - - - - - - - 30

   b. Initialization - 30

   c. Results - 31

   d. Discussion - 31

7. Full Dynamic Model Test - - - - - - - - - - - - - - - - - - - 35

   a. Procedure - 35

   b. Aerosol Results - 36

   c. Mixed Layer Dynamics - - - - - - - - - - - - - - - - - - - 36

8. Conclusions - 43

List of References - 45

Distribution List - 47

LIST OF TABLES

I. Meteorological surface layer data for the CEWCOM-78 analysis period. T_s is the sea-surface temperature and T the air temperature. These are four-hour averages of half-hourly observations - - - - - - - - - - - - - - - 28

II. Entrainment velocity, W_e, and divergence for the analysis period - 29

III. Sea salt aerosol surface volume flux in $\mu m^2/cm^2/s$, as a function of wind speed (m/s) and particle radius (μm) at S = 0.8 - 30

IV. A comparison of Deardorff (1976), W_e, Stage and Businger (1981), W_e', entrainment rates for the initial conditions at each of the 12-hour analysis periods - - - - - - - 41

LIST OF FIGURES

Fig. 1 Height dependence of aerosol volume and relative humidity above the ocean. The curve labeled V is the ambient aerosol total volume ($\mu m^3/cm^3$), the curve label V_o is the volume corrected to 80% reference humidity. The open circles represent the equivalent V_o from the WMK model (Eq. 1) - - - - - 11

Fig. 2 Aerosol volume spectrum, $dV/dr = V(r)$, at $r = 5$ μm as a function of wind speed, u. The circles represent average values obtained from measurements in the North Atlantic with the standard deviation shown as brackets. The dashed line is the WMK model and the solid line is a similar model taken from earlier measurements in the Atlantic - - - - - - - 12

Fig. 3 Marine boundary layer well-mixed structure in a two layer idealization. The height of the mixed layer is h. θ_v is the virtual potential temperature, Q the water vapor density and ρ the density of air - 15

Fig. 4 Height dependence of continental, V_c, and sea-salt, V_s, aerosols in the mixed layer model. As shown, the aerosol volumes are represented at fixed humidity - - - - - - - - - - 20

Fig. 5 Location of the CEWCOM-78 experiment in coastal southern California. The line indicates the track of the R/V ACANIA - 23

Fig. 6a Composite radiosonde measurements of θ_v at 5/19, 1700 local time - 24

Fig. 6b Composite radiosonde measurements of θ_v at 5/20, 0500 local time - 25

Fig. 6c Composite radiosonde measurements of θ_v at 5/20, 1700 local time - 26

Fig. 6d Composite radiosonde measurements of θ_v at 5/21, 0500 local time - 27

Fig. 7 Ratio of ambient aerosol volume at the hour indicated to the volume at the beginning of the period, $V_{sm}(r,t)/V_{sm}(r,o)$. The open circles are the mixed layer dynamic model, the X's are the measurements and the solid circles are the WMK model. The mixed layer model and measurements were normalized by the initial value of the data. The WMK ratio was obtained by normalizing with the WMK model value obtained from the initial wind speed and relative humidity - - - - - - 32

Fig. 8 Initial (circled X's) and final (X's) measured aerosol spectra. The mixed layer model spectrum is the open circles and the WMK model spectrum is the solid circles - - - - - - - 33

Fig. 9 Temporal evolution of the aerosol volume at r = 0.8 μm, 5 μm and 15 μm over the 38 hour period beginning at 1700 local time on 5/19. The open circles are the full mixed layer model, the solid circles are the WMK model and the X's are the data - 37

Fig. 10 Entrainment rate (W_e) and mean vertical motion (W) are on the upper scale and the mixed layer depth (h) is on the lower scale. The symbols are defined in the graphs. The discontinuities in the model results are due to re-initialization at 12 hour intervals - - - - - - - - - - - - - - - - - - 39

Fig. 11 Temporal evolution of the well mixed meteorological variables θ and q. The surface data were measured on the R/V ACANIA - 40

Fig. 12 Similar to Figure 11 but for the ambient saturation ratio S at Z = 10 m - 42

1. Introduction

This is one of a series of reports that describes the Naval Postgraduate School's (NPS) approach to marine atmospheric boundry layer (MABL) modeling. The basics of the approach and the status of modeling and parameterization of the pertinent physical processes are given in Fairall et al. (1981). The utility of the model for tactical use and initial validation of the model are given in Davidson et al. (1982). In this report we describe the use of the model for analysis and prediction of the aerosol content of the MABL.

Interest in marine aerosols has increased recently because of their contribution to the scattering and absorption of light. Estimating these influences on electro-optical (EO) system performance has been emphasized in several studies such as Barnhardt and Streete (1970). An aerosol size of interest is that associated with locally generated sea salt because of its effects on IR as well as visible wavelengths. Measured distributions in the sea salt size range show several orders of magnitude variability, and considerable effort has been expended to normalize these measurements by correcting appropriately for relative humidity and wind speed. These two meteorological quantities are considered because of their role in generation (wind), transport (wind), and growth (relative humidity) of aerosols.

Both empirical and theoretical bases exist for formulating expressions for equilibrium aerosol distributions. Past quantifications of the dependence of equilibrium distributions on relative humidity were made by Fitzgerald (1975). Dependence on turbulent transport was considered by Toba (1965), and dependence on surface generation by Chaen (1973). However, aerosol models in use today utilize only parameterizations of the effects

of relative humidity and wind speed on the equilibrium aerosol distributions (e.g., Wells et al, 1977). Recent evaluations have shown that these models are limited to mean (that is, the average aerosol density encountered at a given wind speed and humidity) distributions (Fairall et al, 1982). These models are inherently limited because some processes in the atmospheric mixed layer which affect aerosol concentrations are not considered.

In this study we will present an approach for including meteorological descriptions which encompass processes and structures of the whole marine atmospheric boundary layer. The top of the boundary layer is capped by the marine inversion where entrainment of overlying air takes place. Because entrainment mixes clear (non-marine) air into the marine layer this process is as important as surface layer aerosol fluxes in determining the equilibrium concentration. The primary goal of our examination will be to incorporate in aerosol descriptions recently established features of the inversion capped marine boundary layer. The features will be presented in terms of an integrated slab model. Such a model is especially desirable since the only input parameters needed are routine meteorological observations.

2. Description and Evaluation of Existing Aerosol Models

A representative example of current models for estimating equilibrium aerosol distributions is that formulated by Wells et al (1977). Their formulation was modified by investigators in the Navy Electro-Optical/Meteorology Program (Hughes, 1980). The number density spectrum, n(r), of the sea salt component is described in the modified version as

$$n(r) = (r/a)\ 1.62\ (C_1+C_2 v^{\delta})/F e^{-Z/h_o F - 8.5(r/a)^{\gamma}}, \qquad (1)$$

where

r = the particle radius in μm

u = the wind speed

$v = 0.5$ for $u \leq 4$ m/s ,

$v = u - 3.5$ for $u > 4$ m/s ,

$F = 1 + (v/60)^3$,

$\gamma = 0.384 - 0.00293\ v^{1.25}$,

Z = height above sea surface, m ,

h_o = scale height, m (800 m for $Z < 1000$ m) ,

$a = 0.81 \exp(0.066S/(1.058 - S))$,

$S = H/100$, (H is relative humidity in per cent).

The other constants are

v(m/s)	C_1	C_2	δ
$v \leq 7$	350	1000	1.15
$v > 7$	0	6900	0.29

The relative humidity growth factor, a, has the form suggested by Fitzgerald (1975). The height dependence is exponential, with the scaling height, h_o, being a function of wind speed as suggested by Toba (1965). The leading term $(C_1+C_2\ v^{\delta})$ corresponds to local generation and has a pow

law dependence on wind speed. This particular version is referred to as the WMK model.

Examination of a considerable amount of data obtained in the Northeast Atlantic and the Eastern Pacific indicates that Eqn 1 is incomplete. Figure 1 shows the height dependence of total aerosol volume from a sample set of Eastern Pacific data. The three aerosol profiles correspond to (1) the observed sea salt aerosol volume, V, (2) the observed sea salt aerosol volume adjusted to 80% relative humidity equilibrium sizes, V_o, and (3) the WMK predicted volume adjusted to 80% (open circles). These data were obtained under forced convective conditions and with active local production. In order to examine only the height dependence issue, observed and model values have been matched at the surface to remove the production influence. It is clear from the figure that within the mixed layer the observed decrease of aerosol volume with height is less than that predicted by Eqn 1. The surface generated aerosols appear to be well-mixed below the inversion when normalized to remove the influence of relative humidity. This has also been observed by other investigators (Blanchard and Woodcock, 1980; Hughes, 1980; Johnson and Hering, 1981). Aerosol volume corrected for relative humidity can be considered to be reasonably well mixed from the inversion down to approximately the 10-meter level for these conditions.

Evidence supporting our assertion that existing scaling of production effects are reasonable only for mean or climatological purposes appears in results obtained in the Northeast Atlantic. This point is illustrated in Fig. 2 where normalized measured aerosol volume densities at $r = 5$ μm and the corresponding prediction from Eqn 1 are compared. The values and trends in the predicted and mean results are in reasonable agreement. However, the standard deviation is so large that, at a given time, only 67% of the

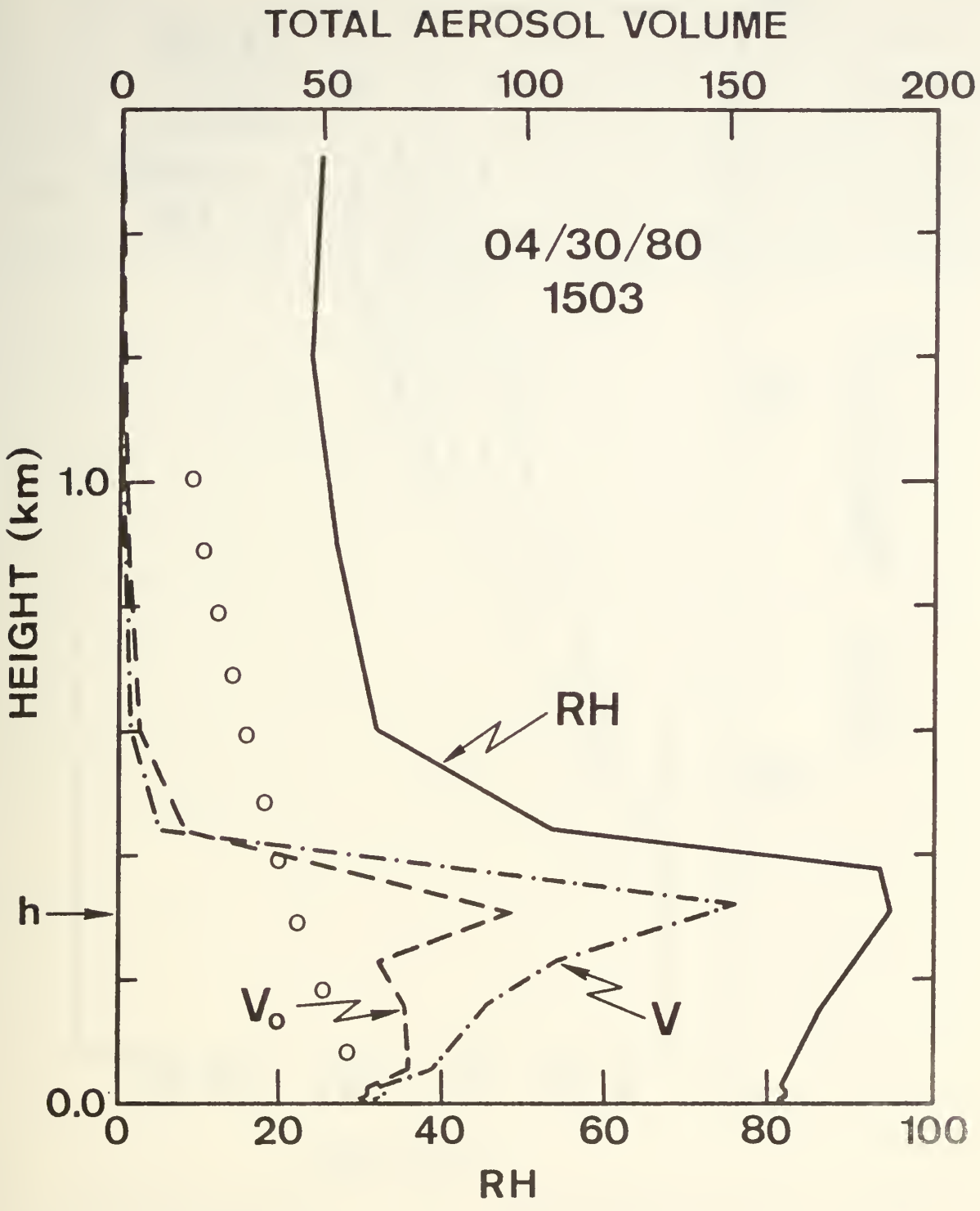

Fig. 1 Height dependence of aerosol volume and relative humidity above the ocean. The curve labeled V is the ambient aerosol total volume ($\mu m^3/cm^3$), the curve label V_o is the volume corrected to 80% reference humidity. The open circles represent the equivalent V_o from the WMK model (Eq. 1)

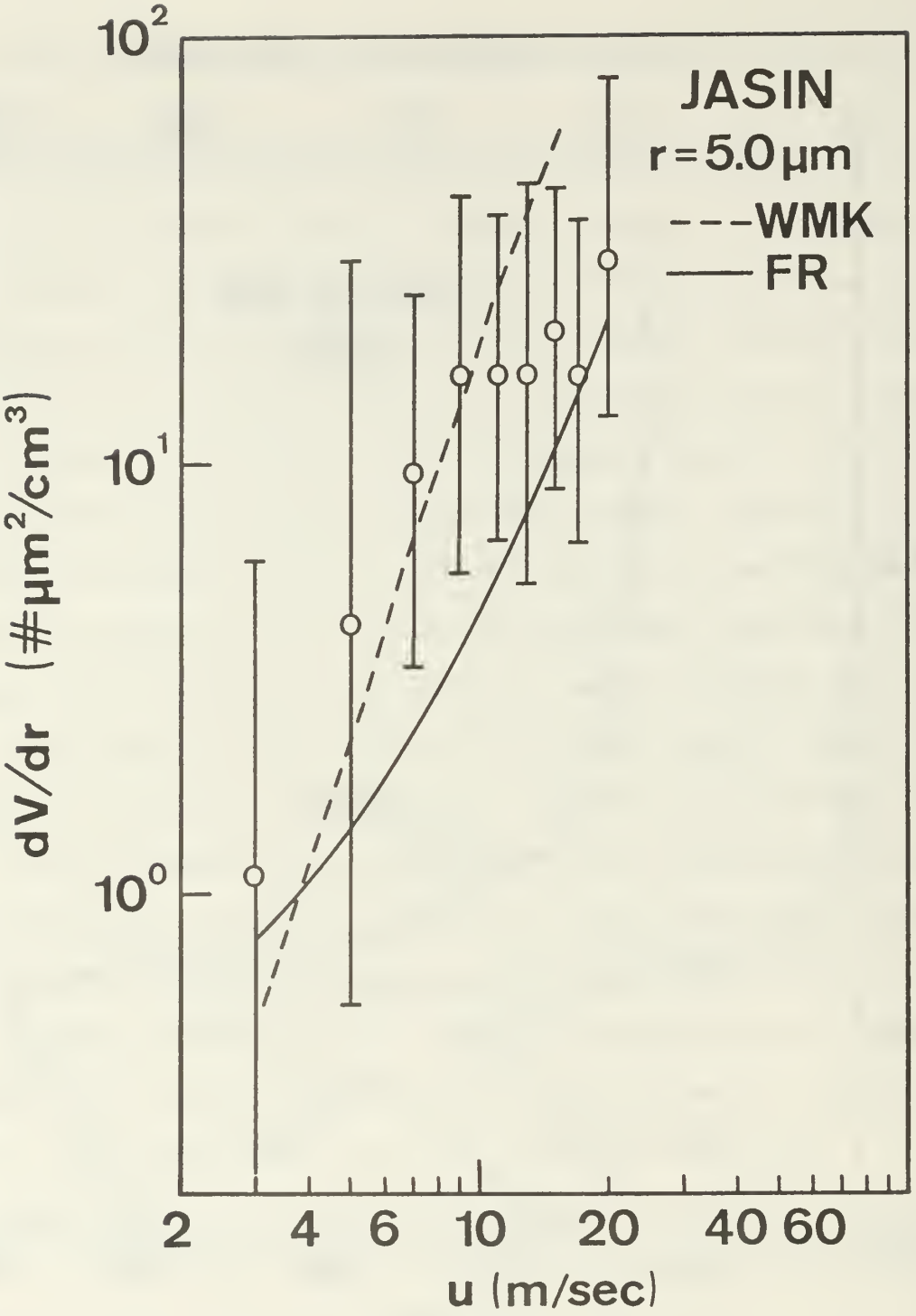

Fig. 2 Aerosol volume spectrum, dV/dr = V(r), at r = 5 μm as a function of wind speed, u. The circles represent average values obtained from measurements in the North Atlantic with the standard deviation shown as brackets. The dashed line is the WMK model and the solid line is a similar model taken from earlier measurements in the Atlantic

observed aerosol distributions will be within a factor of three of the average. The point is that no matter how accurately the model predicts the average aerosol density at a given wind speed and relative humidity, the factor of three for the RMS variation cannot be eliminated without considering more parameters than instantaneous wind speed and relative humidity.

3. Boundary Layer Model

The prime feature characterizing the marine atmospheric boundary layer is that it is convectively mixed, and hence homogeneous, up to a height h, where it is capped by an inversion. The mixed layer is cool and moist relative to the overlying stable layer (shown in Fig. 3).

The fundamental assumption of existing models of the boundary layer is that well-mixed properties remain well mixed when undergoing evolutions in time. If the value of any well-mixed property, X, were to change solely because of turbulent fluxes at the top and bottom boundaries and uniform horizontal advection, and if X remains well mixed after the change, then it follows that the vertical flux profile, $\langle W'X' \rangle$, must be linear. For this case the appropriate balance expression for the local change of X is (Lilly, 1968)

$$dX/dt + V_H \cdot \nabla X = (\langle W'X' \rangle_o - \langle W'X' \rangle_i)/h \ , \qquad (2)$$

where $V_H \cdot \nabla X$ is the horizontal advection, the brackets represent a suitable average for the responsible turbulent scales, and subscripts o and i refer to surface and inversion values, respectively.

Difficulties in making measurements of the fluxes at the inversion and evaluating the horizontal advection make Eqn 2 impractical for single location observations without further simplification and scaling. The horizontal advection term is excluded in the following discussion not because it is necessarily negligible but simply to limit the scope of this paper. The surface flux is easily calculated using the bulk aerodynamic method. This leaves the flux at the inversion to be parameterized in order for Eqn 2 to be a usable balance expression for single station assessments.

The relationship between the equivalent flux property at the inversion, $\langle W'X' \rangle_i$, the rate of change of the mixed layer depth (dh/dt), the mean

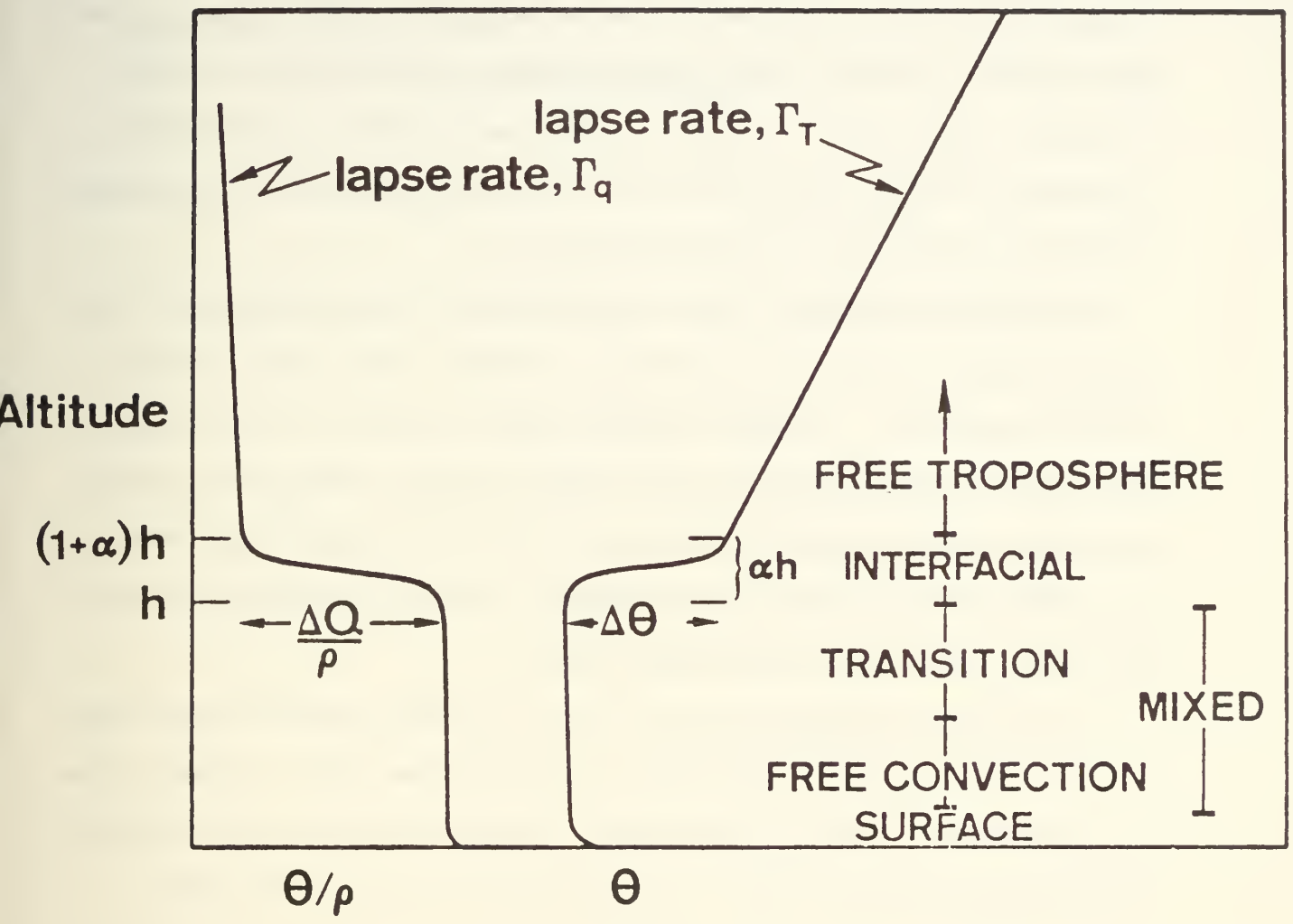

Fig. 3 Marine boundary layer well-mixed structure in a two layer idealization. The height of the mixed layer is h. θ_v is the virtual potential temperature, Q the water vapor density and ρ the density of air

vertical motion, W, the entrainment velocity, W_e, and the "jump" in X, ΔX, at the inversion is:

$$dh/dt = W + W_e \ , \tag{3a}$$

$$\langle W'X' \rangle_i = - W_e \ \Delta X \ . \tag{3b}$$

The utility of these expressions depends on the capability to estimate the quantity W_e from bulk parameters. An estimate of the $\langle W'X' \rangle_i$ term in Eqn 3 can be made if changes of the inversion height and subsidence rates are known ($W_e = dh/dt - W$). As such, it would not be useful for prediction since one uses W_e to predict dh/dt, but it could be applied to analytically explain contributions to observed changes in X.

All integrated schemes relate the availability and consumption of turbulent kinetic energy at the inversion to surface, cloud regime, and inversion parameters. Turbulent kinetic energy available for entrainment is derived from surface layer and cloud region buoyancy fluxes and mechanical turbulence associated with surface layer and inversion layer wind shears. The effectiveness of the available energy in driving entrainment depends on the static stability of the inversion layer.

The simplest formulation for W_e is for the cloud free zero-order model (Fig. 3) where the static stability is scaled by the jump in virtual potential temperature. The available kinetic energy is assumed to be a fraction of the surface buoyancy flux. The expression for W_e is (Lilly, 1968)

$$W_e = f \langle W'\theta_v' \rangle_o / \Delta\theta_v \ , \tag{4}$$

where suggested values of f have ranged from .1 to .3.

The complexity of parameterizations of this type increases when cloud region buoyancy is included and when more realistic structures are used for the inversion zone. Deardorff (1978) and Stage and Businger (1981) are suggested for more complete descriptions of the scaling procedures. In all

cases, however, a useful scaling velocity for the entrainment rate is the convective mixing velocity,

$$W_* = (gQ_o Z_i/T)^{1/3} , \qquad (5)$$

where $Q_o = \langle W'\theta'_v \rangle_o$, $Z_i = (1 + \alpha)h$ is the inversion height, T the absolute temperature, and g the acceleration due to gravity. The equivalent expression to Eq. 4 has the form

$$W_e/W_* = fW_*^2/(gZ_i \Delta\theta_v/T) . \qquad (6)$$

4. Aerosol Considerations in a Well-Mixed Model

The first step in applying the mixed layer model to aerosol descriptions is the establishment of the well-mixed parameters. In the case of temperature (clear sky) it is the virtual potential temperature; in the case of humidity it is the water vapor mixing ratio. Although a given aerosol particle may vary in size due to changes in ambient relative humidity, the salt particle spectrum is conserved (because of the lower number concentrations of sea salt aerosols, coalescence can generally be neglected). Thus, the well-mixed property for aerosols is the dry size spectrum mixing ratio, or equivalently, the aerosol spectrum mixing ratio at some reference relative humidity. We will consider the aerosol volume spectrum

$$V(r) = 4/3\pi\, r^3 n(r) \ , \tag{7}$$

where $n(r) = dN/dr$ is the number density spectrum.

We shall define $V(r)$ as the volume of aerosol particles per cm^3 per radius increment at STP and at the reference saturation ratio, $S_o = 0.8$. At some height in the mixed layer, where the local ambient air density is ρ and the saturation is S, the aerosol volume spectrum is

$$V'(r_s(S)) = V(r_o)\ g^2(S)\rho/\rho_o \ , \tag{8}$$

where ρ_o is the density of air at the surface, r_o and r_s the particle radii at the reference and ambient saturation

$$r_s = r_o g(S) \ , \tag{9}$$

and $g(S)$ is the humidity growth factor

$$g(S) = .81 \exp(0.066\ S/(1.058-S)) \ . \tag{10}$$

Note that ρ/ρ_o is included to maintain a constant mixing ratio.

The next step in applying the mixed layer model to aerosols is to recognize that all aerosols do not originate locally. Both above and below

the inversion, aerosols are advected into the local region. In terms of aerosol density, entrainment acts as an aerosol flux (out of the boundary layer) because the aerosol concentrations above and below the inversion are different. In the mixed layer model the entrainment acts on the jump across the inversion and the flux of a scalar property is

$$\langle W'X' \rangle_i = -W_e \Delta X = -W_e(X_p - X_m) \ , \qquad (11)$$

where X_p is the quantity just above the inversion and X_m is the quantity just below the inversion.

With aerosols we find it useful to consider two components as distinguishable from each other. The total aerosol volume is the sum of the surface generated salt component, V_s, and the background (continental) component, V_c (Figure 4); then

$$V_m = V_{sm} + V_{cm} \ , \qquad Z < h \qquad (12a)$$

$$V_p = V_{cp} \ , \qquad Z > h \qquad (12b)$$

where we have assumed $V_{sp} = 0$.

At this point Eqn 3 can be applied to each component

$$h(dV_{sm}/dt) = \langle W'V_s' \rangle_o - (W_e + W_{km})V_{sm} \ , \qquad (13a)$$

$$h(dV_{cm}/dt) = W_e(V_{cp} - V_{cm}) - W_{km} V_{cm} + W_{kp} V_{cp} \ , \qquad (13b)$$

where we have neglected horizontal advection, assumed negligible local production for the continental component ($\langle W'V_c' \rangle_o = 0$) and included the Stokes gravitational fallout term W_k (Wu, 1979). The fallout rates above and below the inversion are different because of the change in the aerosol spectra caused by the humidity growth factor. The Stokes velocity is calculated from

$$W_k = 2g(\rho_w - \rho)r_o^2 g^2(S)/(9E\rho) \ , \qquad (14)$$

where ρ_w is the density of the droplet, g the gravitational acceleration and E the kinematic viscosity of air. Since the rate of change of th

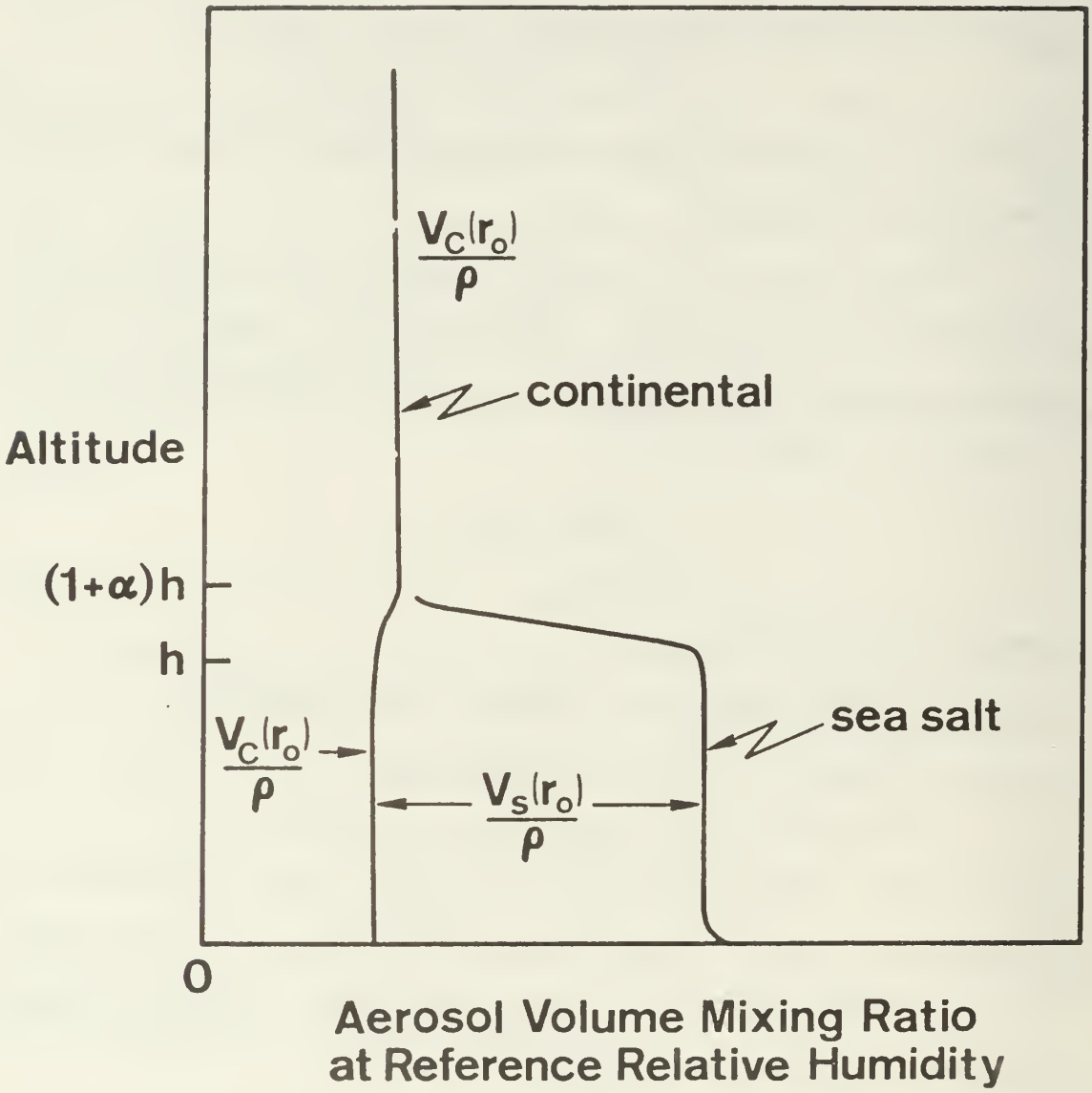

Fig. 4 Height dependence of continental, V_c, and sea-salt, V_s, aerosols in the mixed layer model. As shown, the aerosol volumes are represented at fixed humidity

continental component (dV_{cm}/dt) due to mixed-layer processes is often small compared to the advective effects, no attempt will be made to investigate Eqn 13b. The actual process of determining the separate components of a measured aerosol spectrum presently relies on the fact that virtually all particles with radii less than 0.1 μm are of "continental" origin (Fairall et al, 1982).

5. Marine Boundary Layer Experiment

The previously described aerosol balance expression will be evaluated with aerosol and atmospheric mixed layer measurements made off the U.S. West Coast. They were made during the Cooperative Experiment on West Coast Oceanography and Meteorology (CEWCOM-78) which was conducted from 25 April to 23 May 1978 by several U.S. Navy sponsored groups. Measurements were made from the research vessel ACANIA and several shoreline radiosonde stations. The general area of the experiment is shown in Figure 5. Descriptions of synoptic scale conditions influencing the Los Angeles basin throughout the entire CEWCOM-78 period have been presented by Rosenthal et al (1979). For this evaluation we chose a period, 20-21 May, toward the end of the experiment.

The 20-21 May period was one of increasingly maritime conditions in the Los Angeles basin due to onshore flow caused by the development of a thermal trough over Southern California. This thermal trough developed in conjunction with the intensification of a Pacific high located west of Washington state.

Mixed layer changes during this period were controlled by the following factors: 1) widespread subsidence was occurring over a uniform mixed layer, 2) prevailing onshore flow reduced the effect of local land/sea circulations, 3) overcast stratus-stratocumulus contributed to the entrainment at the top of the layer, and 4) advection was not a significant factor in local changes of mixed layer depths.

Deepening of the marine, or mixed, layer during the period is evident in an acoustic sounder record which was obtained on the R/V ACANIA and from composite profiles constructed from radiosondes launched at shoreline and ship locations (Fig. 6). The acoustic sounder record and the composite pro-

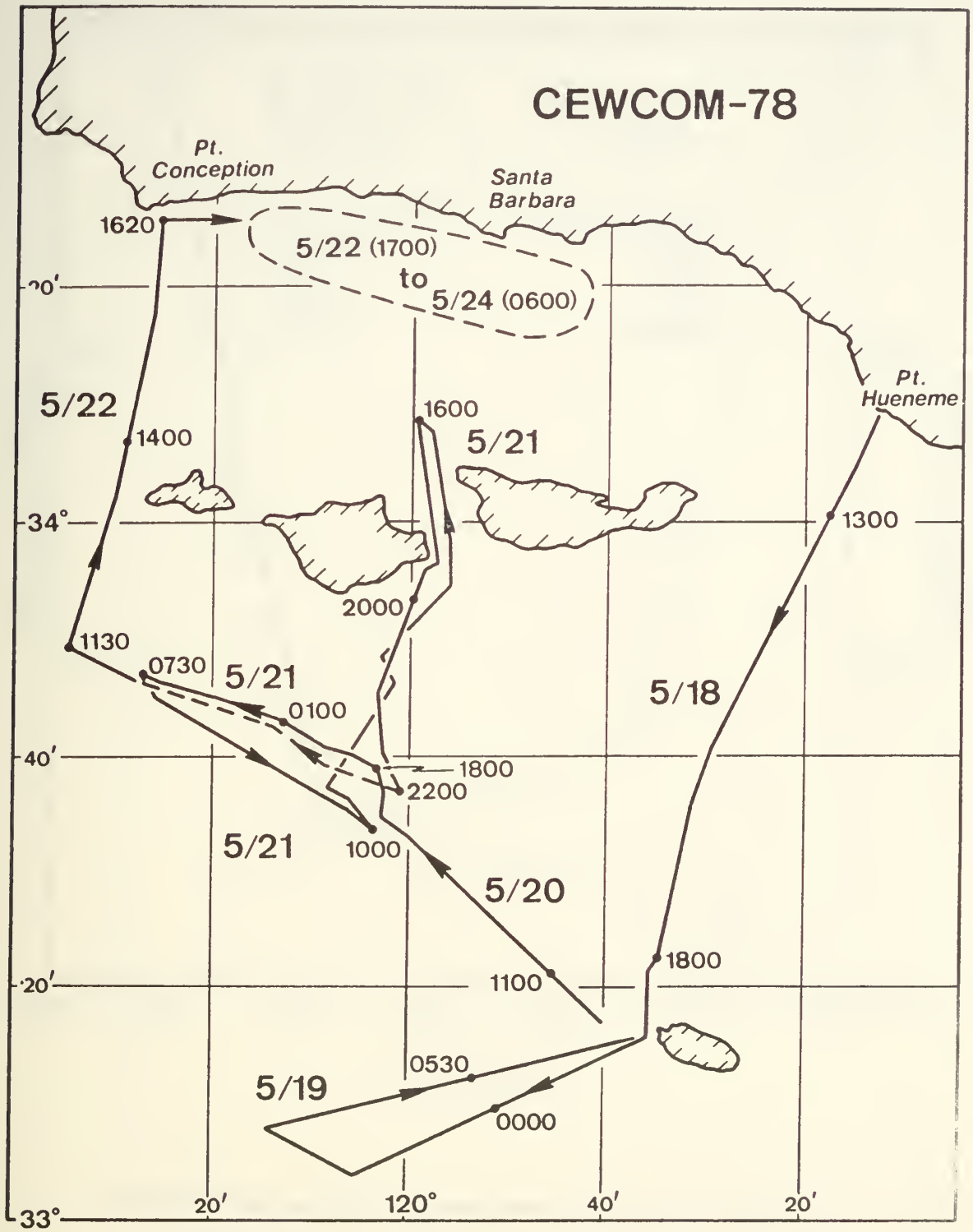

Fig. 5 Location of the CEWCOM-78 experiment in coastal southern California. The line indicates the track of the R/V ACANIA

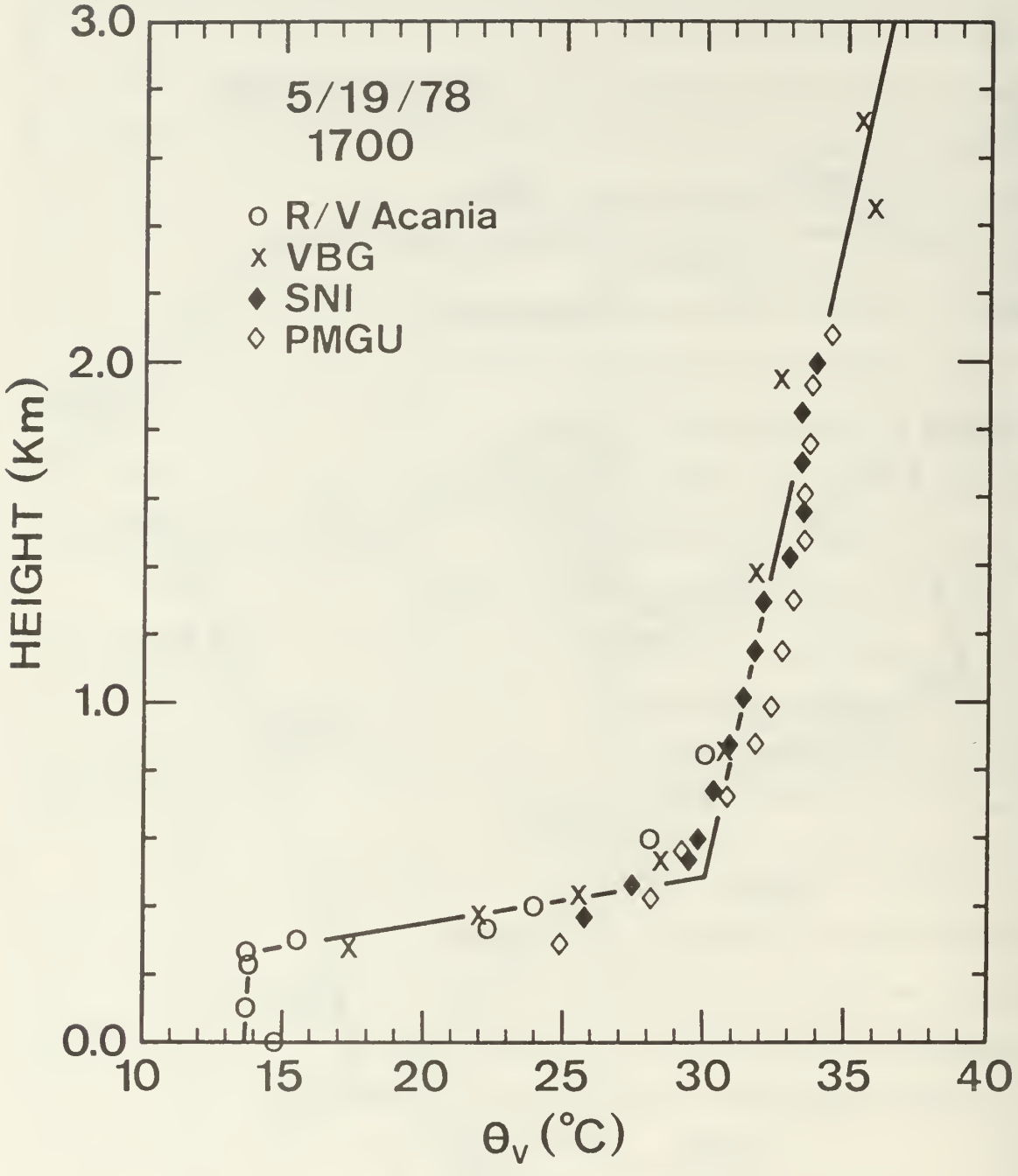

Fig. 6a Composite radiosonde measurements of θ_v at 5/19, 1700 local time.

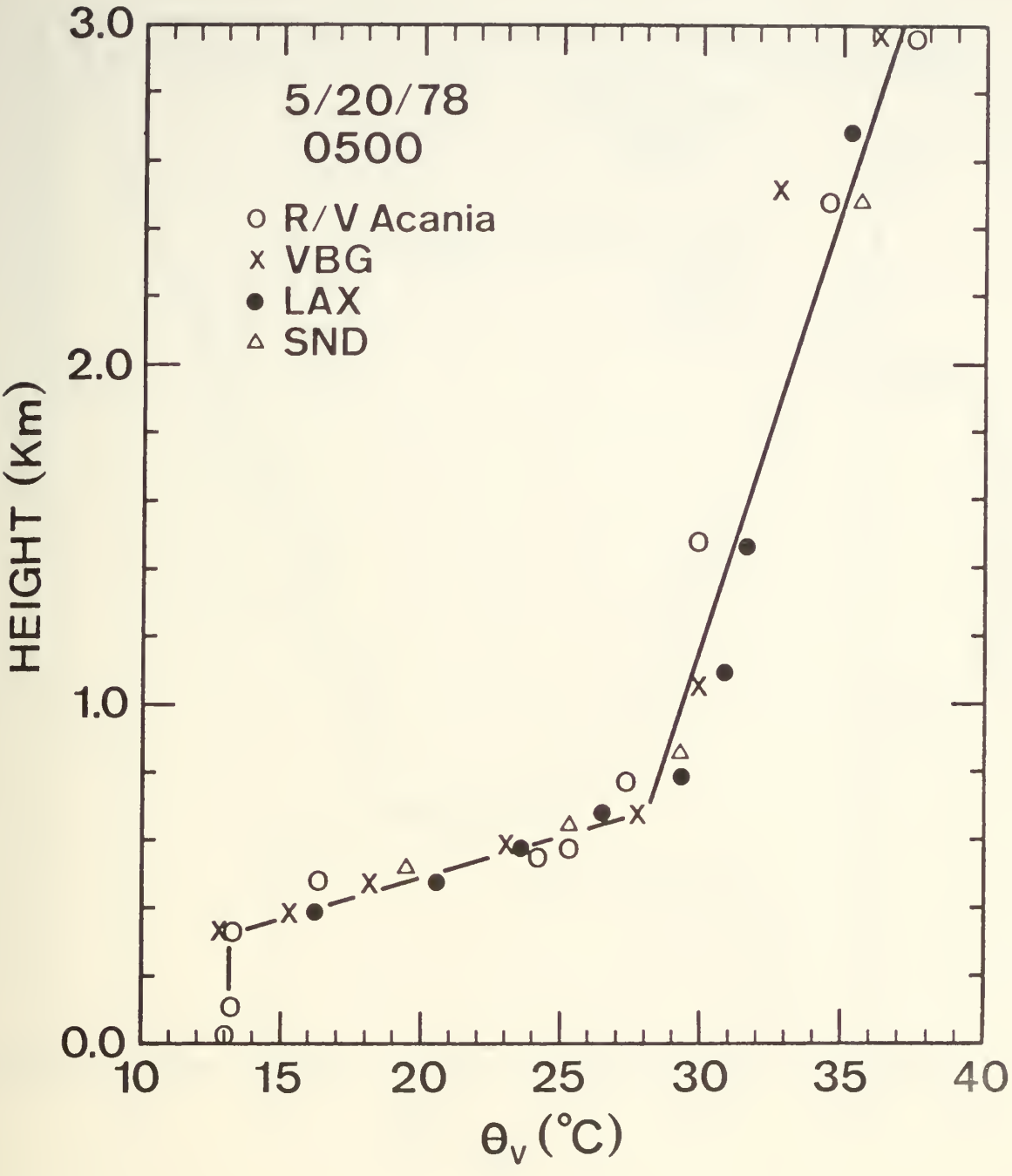

Fig. 6b Composite radiosonde measurements of θ_v at 5/20, 0500 local time

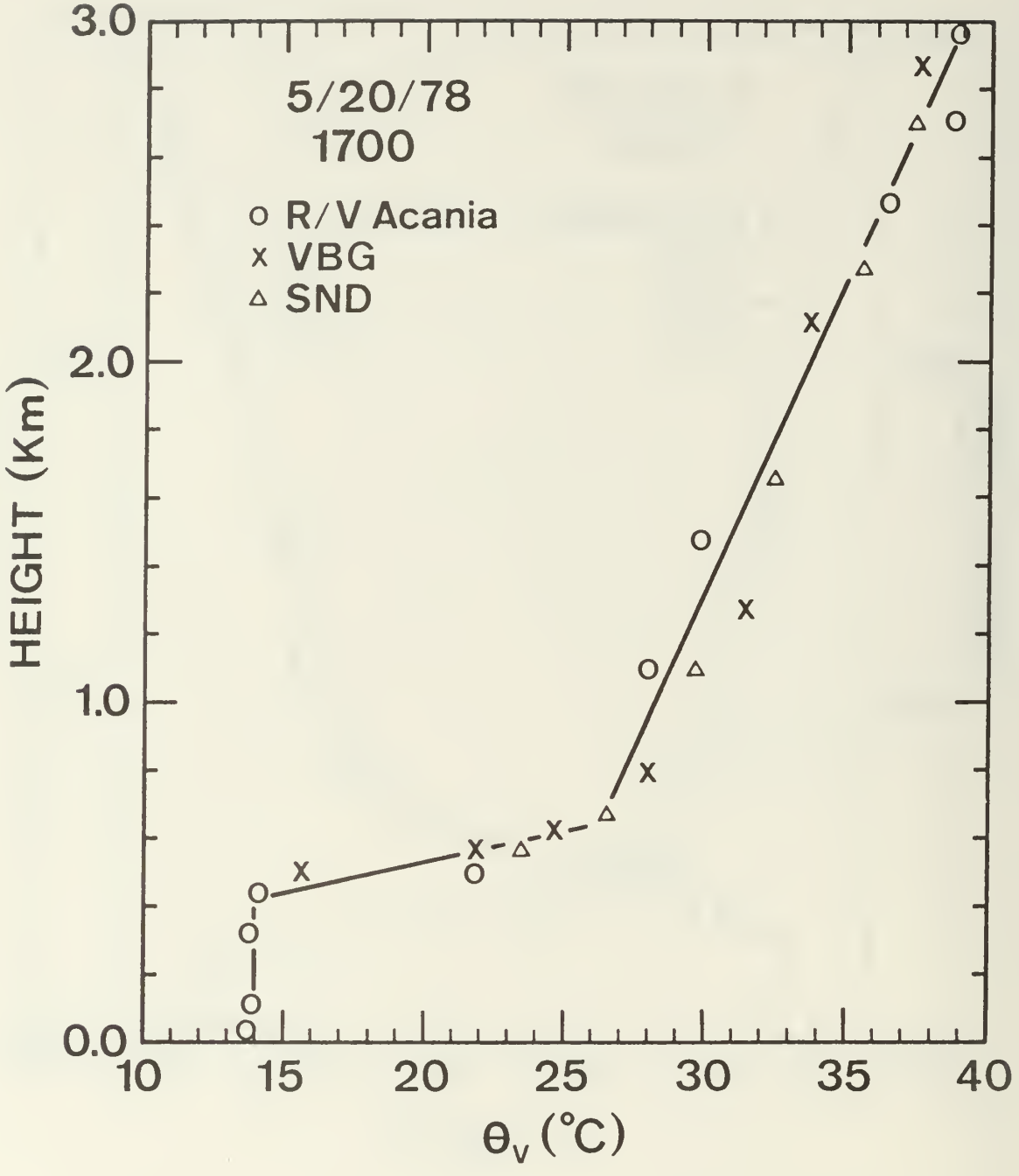

Fig. 6c Composite radiosonde measurements of θ_v at 5/20, 1700 local time

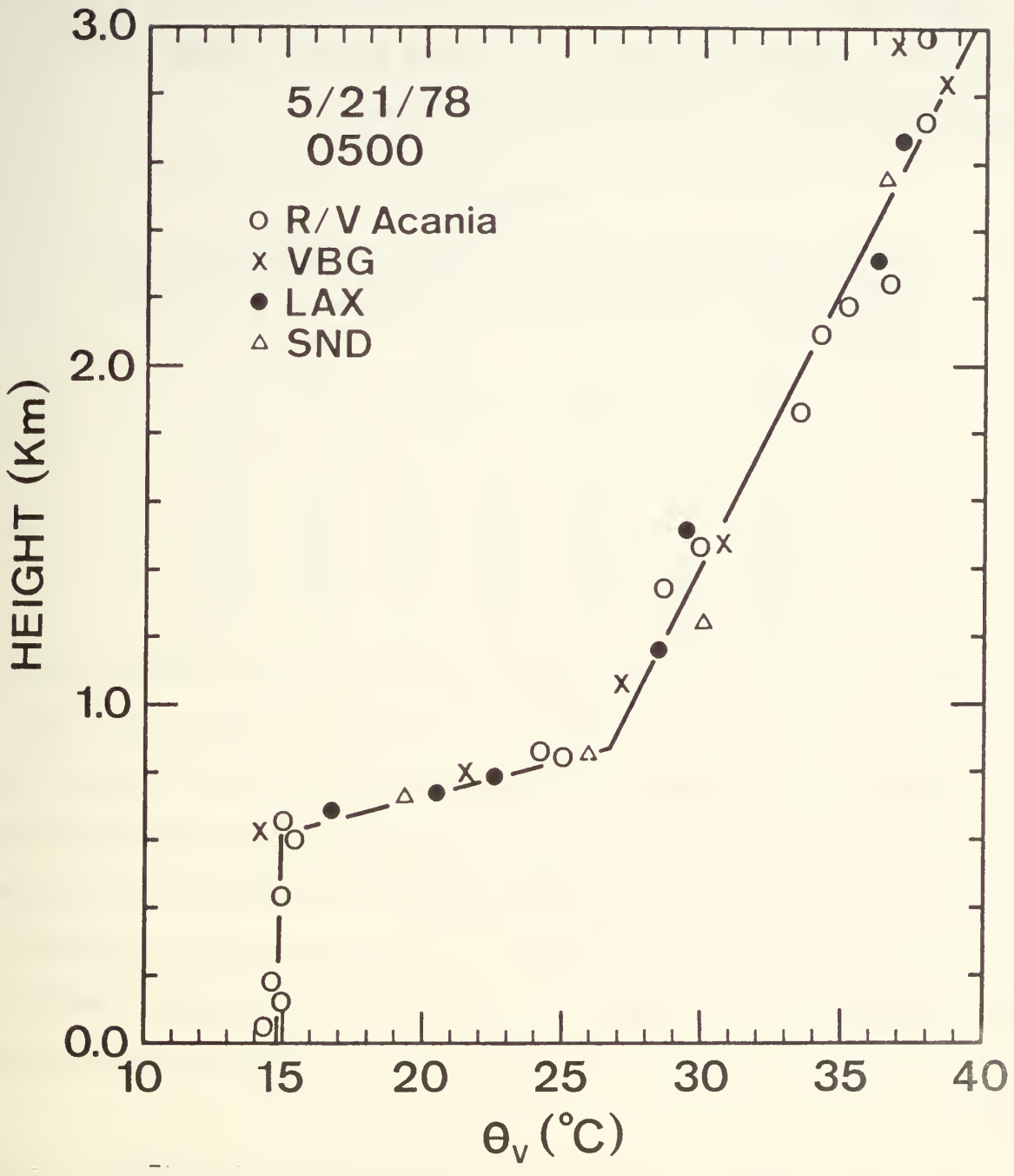

Fig. 6d Composite radiosonde measurements of θ_v at 5/21, 0500 local time.

files indicate that the mixed layer depth was nearly the same at all stations and changed uniformly.

Measurements from the R/V ACANIA provided information on the surface layer wind, temperature, humidity and aerosol spectrum. These data are summarized in Table I for the period of interest.

Table I

Meteorological surface layer data for the CEWCOM-78 analysis period. T_s is the sea-surface temperature and T the air temperature. These are four-hour averages of half hourly observations.

Date	Time	u(m/s)	S	T_s(C)	T(C)	h(m)
5/20	1300	7.9	.86	14.0	12.3	425
5/20	1700	8.7	.82	14.4	12.6	435
5/21	2100	9.8	.87	13.7	12.1	385
5/21	0100	9.2	.88	13.1	12.0	448
5/21	0500	8.2	.83	13.0	12.0	615

Practical application of a mixed layer model requires parameterization of the entrainment rate, W_e. However, in Section 4 we wish to test only the aerosol part of the model, not the accuracy of various entrainment predictions. Therefore, the entrainment rate was directly estimated from the measured evolution of the well-mixed humidity and temperature over the period using the NPS boundary layer model. An entrainment rate was selected that reproduced the evolution of the non-aerosol mean variables (humidity and temperature) and then that entrainment rate was applied to the aerosol evolution.

The vertical motion, W, was calculated using the known changes in h and the values to W_e in Eqn 3a. The divergence, D, was estimated as $D = -W/h$ (Table II).

Table II

Entrainment velocity, W_e, and divergence for the analysis period.

Period	W_e (cm/sec)	Divergence (sec^{-1})
5/20-0500 to 5/20-1700	0.32	7.5×10^{-6}
5/20-1700 to 5/20-2400	0.32	1.3×10^{-6}
5/21-0000 to 5/21-0500	0.38	1.3×10^{-6}

6. Aerosol Model Test

This section is an examination of the ability of Eqn 13a to predict evolutions of sea salt aerosol spectra given ideal estimates of the meteorological parameters. Consequently, measured (as opposed to model parameterized or predicted) values are used for non-aerosol parameters wherever possible. In particular, the wind speed, relative humidity, entrainment rate and boundary layer height for the analysis will be based on actual observations, not model predictions.

a. Aerosol Surface Flux

The evolution of the sea salt component of the aerosols is described by Eqn 13a where h, W_{km} and W_e are given. The only other unknown in the equation is the surface aerosol flux spectrum $\langle W'V_s' \rangle_o$. This quantity has been determined previously from data collected in the Northeast Atlantic during the JASIN experiment, (Fairall et al, 1982) and is given in Table III as a function of wind speed.

Table III

Sea salt aerosol surface volume flux in $\mu m^2/cm^2/s$, as a function of wind speed (m/s) and particle radius (μm) at S = 0.8.

U	r = 0.8	2	5	10	15
6	1.3	1.1	2.5	1.0	0.3
9	4.5	3.1	4.2	3.3	2.3
11	8.2	7.7	11.0	21.0	27.0
13	9.1	9.2	17.0	49.0	48.0
15	11.0	10.0	19.0	72.0	140.0
18	17.0	11.0	24.0	92.0	180.0

b. Initialization

Eqn 13a is a rate equation that relates dV_{sm}/dt to V_{sm}. Consequently the model is used to predict the evolution of V_{sm} subsequent to some initial time for which values of the relevant parameters are known or

assumed. In this example, we will use the values measured at the beginning of the analysis period. If measured aerosol values are not available, the model can be initialized with the equilibrium spectrum obtained from Eqn 13a with $dV_{sm}/dt = 0$:

$$V_{sm}\ (\text{Equilibrium}) = \langle W'V_s' \rangle_o / (W_e + W_{km}) \ . \qquad (15)$$

c. Results

The model was initialized for 1300 PDT on 5/20/78 with the measured spectrum. The evolution of the size spectrum was calculated with half-hour time steps at five particle sizes (r = 0.8, 2, 5, 10 and 15 μm) using the data given in Tables I, II and III. The surface flux used at each wind speed was a log interpolation of the values in Table 3 weighted by the velocity category. The results of the model calculation for three radii are shown in Figure 7 and compared with the measured data and the WMK model at four-hour intervals. Each of the three results plotted is normalized by its own particular value at the start of the analysis period. This was done to avoid biasing the comparison in favor of the mixed layer model which, since it is initialized with the measured data, would tend to automatically predict the correct results more accurately (especially in the earlier periods). The initial and final measured spectra are shown in Figure 8 along with the mixed layer and WMK model predictions.

d. Discussion

The mixed layer aerosol parameterization did a credible job of predicting the aerosol spectum 16 hours after initialization. A log-averaging yielded an average of the predicted to the measured spectra of 0.92 x or ÷ 1.54 ($1.54 = e^{\sigma}$ where $\sigma = 0.43$ is the standard deviation of the log of the ratio and $\langle x \rangle x$ or $\langle x \rangle e^{\pm\sigma} = e^{\langle \ln x \rangle \pm \sigma}$). In this case, the WMK model also performed well with a log-average ratio of prediction to measurement

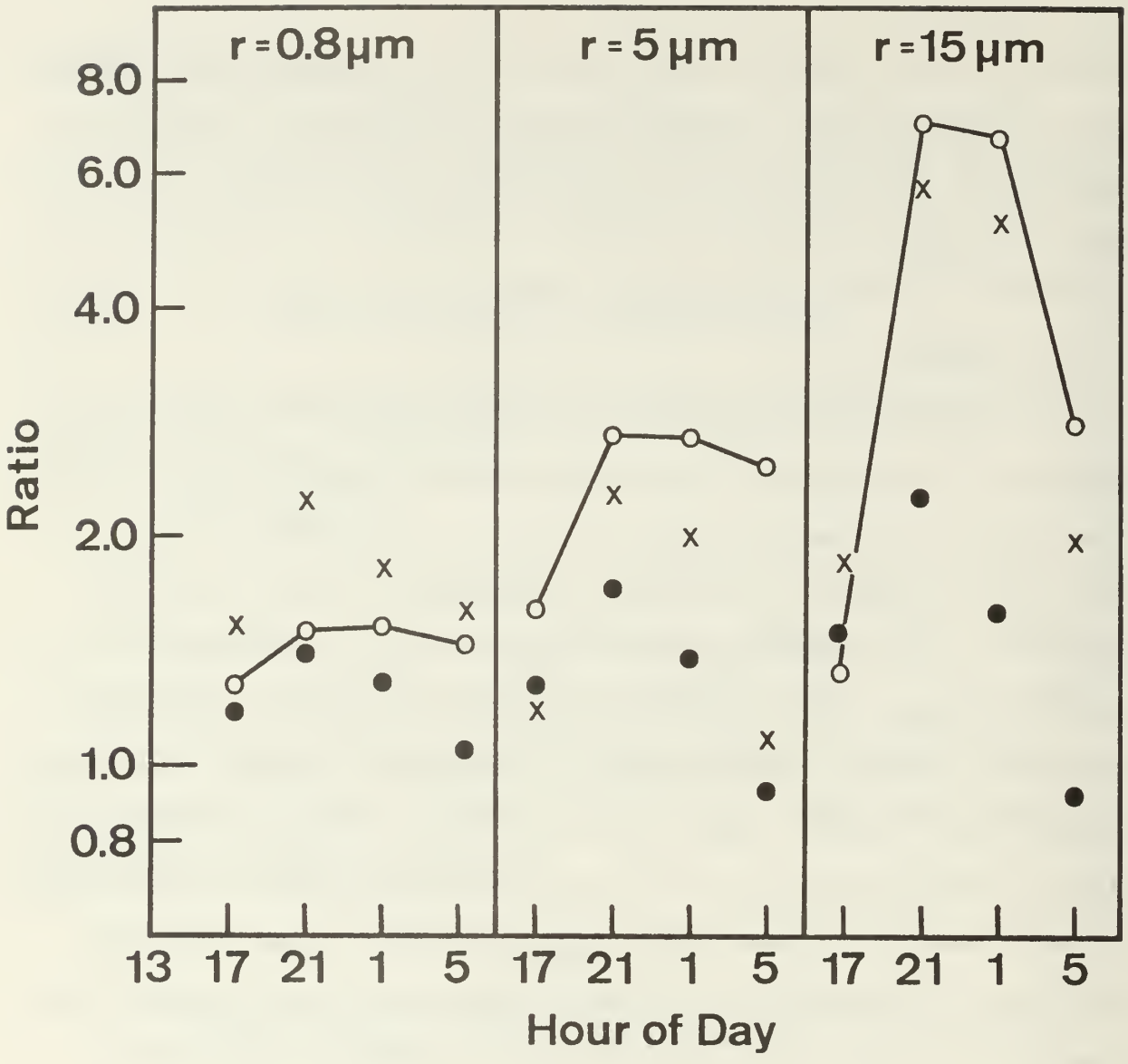

Fig. 7 Ratio of ambient aerosol volume at the hour indicated to the volume at the beginning of the period, $V_{sm}(r,t)/V_{sm}(r,o)$. The open circles are the mixed layer dynamic model, the X's are the measurements and the solid circles are the WMK model. The mixed layer model and measurements were normalized by the initial value of the data. The WMK ratio was obtained by normalizing with the WMK model value obtained from the initial wind speed and relative humidity

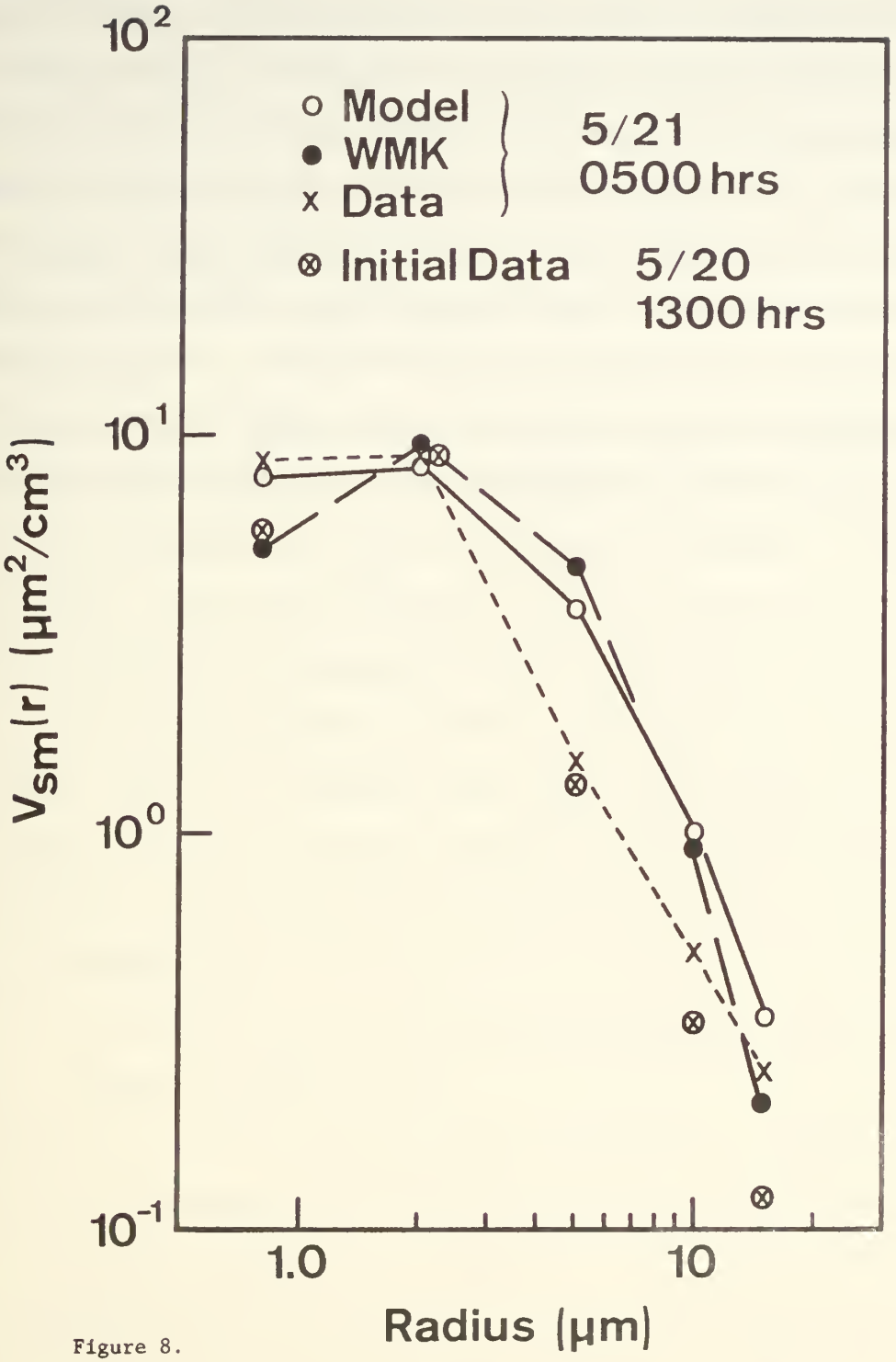

Figure 8.

Fig. 8 Initial (circled X's) and final (X's) measured aerosol spectra. The mixed layer model spectrum is the open circles and the WMK model spectrum is the solid circles

ratios of 1.69 x or ÷ 1.6. This is uncharacteristically good performance for the WMK type of model. In practical application, the mixed layer model will probably not perform this well since several important model parameters (W_e, h, u and S) were not model predicted but obtained from the measurements. This issue will be examined in section 8. Other sources of error (such as advection) will also have an impact. The most important parameter, the surface flux of aerosols (Table III), was based primarily on a single data set obtained in the North Atlantic. Further refinements in the surface flux can, at least potentially, greatly improve the model accuracy. The surface flux data also need to be extended to larger particle sizes.

7. Full Dynamic Model Test

Eqn 13a of Section 4 was tested for a 20-hour time period using measured or directly inferred values of the relevant model parameters. The aerosol model spectrum was initialized at the beginning of the analysis period with the measured spectrum. This section describes a simulation where a complete dynamical, cloud-topped boundary layer model of the Deardorff (1976) type is used to provide the necessary parameters for Eqn 13a.

a. Procedure

The full mixed layer model was run in three 12-hour blocks beginning at 1700 local time on 5/19/78 with subsequent re-initialization of all meteorological variables at the 0000 and 1200 GMT radiosondes (1700 and 0500 local time). The aerosol spectrum was initialized at 1700 on 5/19 using Eqn 15 and was not subsequently reset. The evolution of the aerosol spectum was calculated using Eqn 13a with all parameters taken from the dynamic model output. The measured aerosol data were available for the last 20 hours of the 38-hour model simulation (the final time period was run for 14 hours to cover the last two hours of aerosol data). Other details of relevance are:

1) The surface fluxes were obtained using standard bulk aerodynamic parameterizations.
2) The sea-surface temperature was assigned as the measured value at the beginning of a 12-hour forecast period and assumed to b constant throughout that period.
3) The measured wind speed for a 12-hour period was simplified t two or three continuous linear segments in an effort to simu late an accurate wind speed forecast.

4) The subsidence rate for the start of the test was based on an assumed climatological divergence of $D = 1 \times 10^{-5}$ sec^{-1}. The difference between the predicted and measured values of h at the end of each 12-hour period was used to re-estimate the appropriate subsidence rate for the period. This new subsidence value was then applied to the next 12-hour period.

5) Advection of temperature, water vapor, mixed-layer depth and aerosols were assumed to be negligible.

b. Aerosol Results

Mixed layer model and WMK model aerosol spectra were calculated as described in Sections 5.1 and 4.3. The results are shown in Fig. 9 for the entire 38 hour period. Note that in this case the actual spectral values are plotted rather than the model/initial ratios shown in Fig. 7. The mixed layer model was not a significant improvement over the WMK for this data set. A log-averaging yielded an average ratio of mixed layer model to measured aerosol spectra of 0.76 x or ÷ 2.0 while for the WMK model the ratio was 0.87 x or ÷ 2.2. In other words, the mixed layer model predictions were typically within a factor of 2.0 while the WMK predictions were typically within a factor of 2.2. These can be contrasted with the results of Section 4.4 where, using measured parameters and spectral initialization, the mixed layer model was typically within a factor of 1.5 and the WMK was within a factor of 1.6. Thus, a more realistic application of the model doubled the uncertainty (note that a factor of 1.0 is no uncertainty).

c. Mixed Layer Dynamics

The practical application of the full dynamic model (Section 5) led to an increase of uncertainty in the aerosol prediction from a factor of

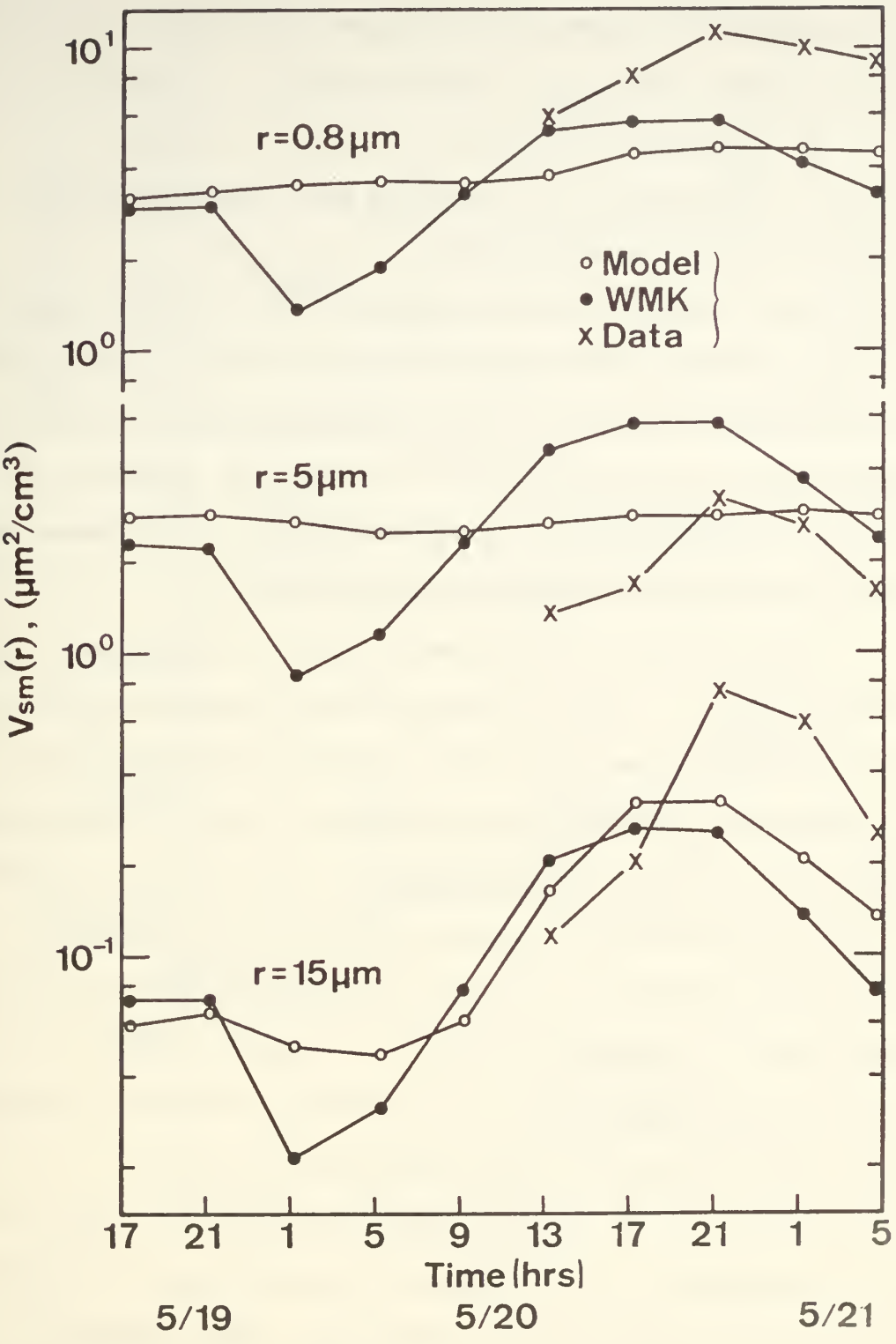

Fig. 9 Temporal evolution of the aerosol volume at r = 0.8 μm, 5 μm and 15 μm over the 38 hour period beginning at 1700 local time on 5/19. The open circles are the full mixed layer model, the solid circles are the WMK model and the X's are the data .

1.5 to a factor of 2. The primary sources of the increase in error are:

1) Use of Eqn 15 for initialization.

2) Model calculations of W_e.

3) Linear smoothing of the wind speed temporal evolution.

4) Model calculation of h.

A comparison of model and measured values of W_e, h and W is shown in Fig. 10. Recall that the model was initialized at 12 hour intervals based on the radiosondes rather than surface based measurements of temperature (θ), humidity (q) and mixed layer depth (h). Whether the substantial differences between the radiosonde and surface based data are due to measurement inaccuracy or a difference in sampling is not known.

The calculation of evolutions of the well mixed θ and q variables is shown in Fig. 11. Since the Deardorff model substantially over-estimated W_e through the analysis period, the model predicted too much warming. This was not only because of the entrainment of too much warm air but also because of the calculated reduction of long wave/cloud-top radiative cooling due to overthinning of the stratus cloud layer by the model. Another factor in the prediction of θ and q was the overestimation of the surface fluxes caused by the use of a sea surface temperature higher than the average for the 12 hour period (the sea surface temperature declined by roughly 0.8 ^{o}C during each 12 hour period).

The tendency of the Deardorff model to overestimate W_e for thin clouds has been discussed by Stage and Businger (1981). They use a slightly different parameterization and find substantially lower values of W_e if Z_c/h is close to one (Z_c is the lifting condensation level). A comparison of W_e estimates of Deardorff (1976) and Stage and Businger (1981) is shown in Table IV.

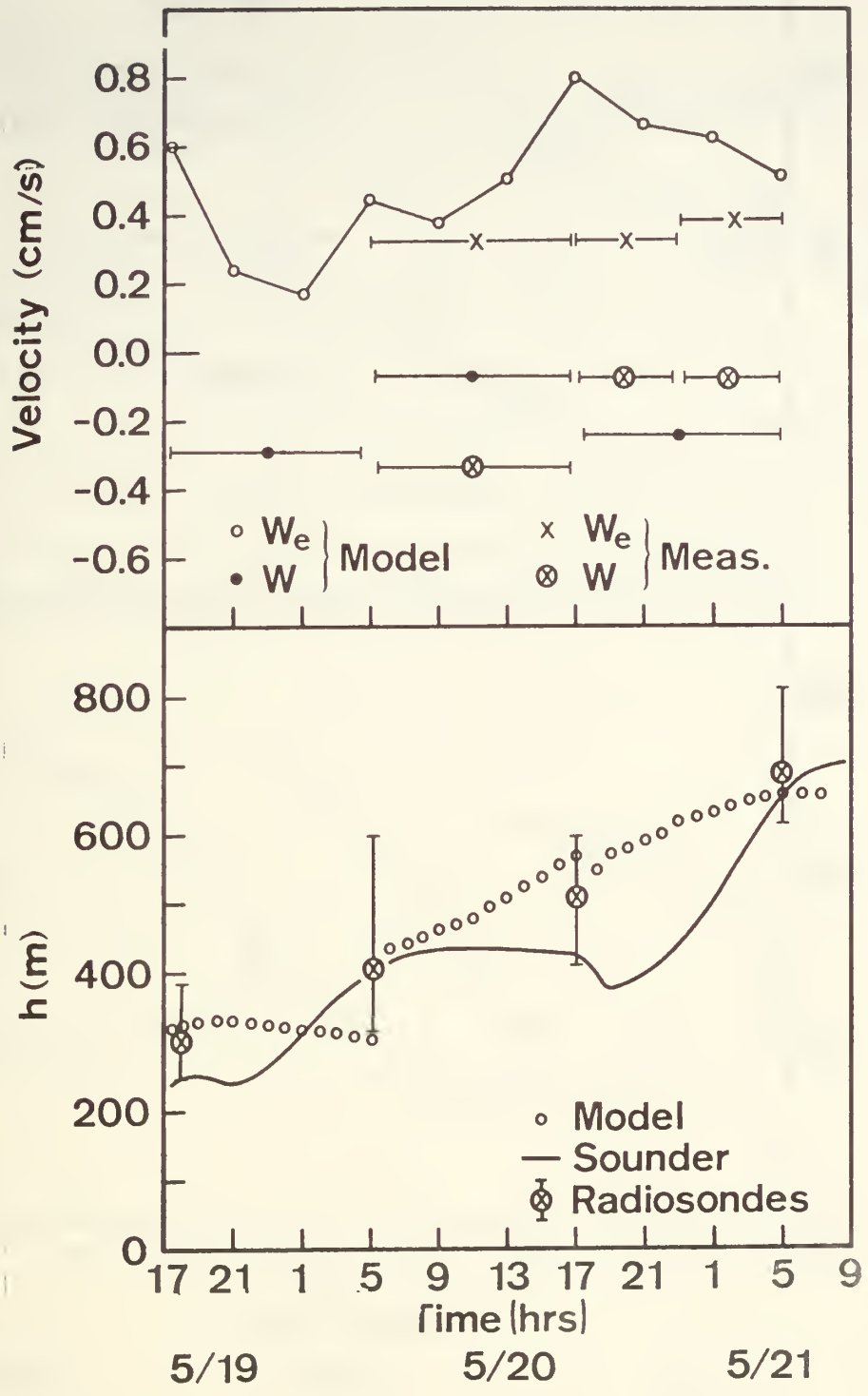

Fig. 10 Entrainment rate (W_e) and mean vertical motion (W) are on the upper scale and the mixed layer depth (h) is on the lower scale. The symbols are defined in the graphs. The discontinuities in the model results are due to re-initialization at 12 hour intervals

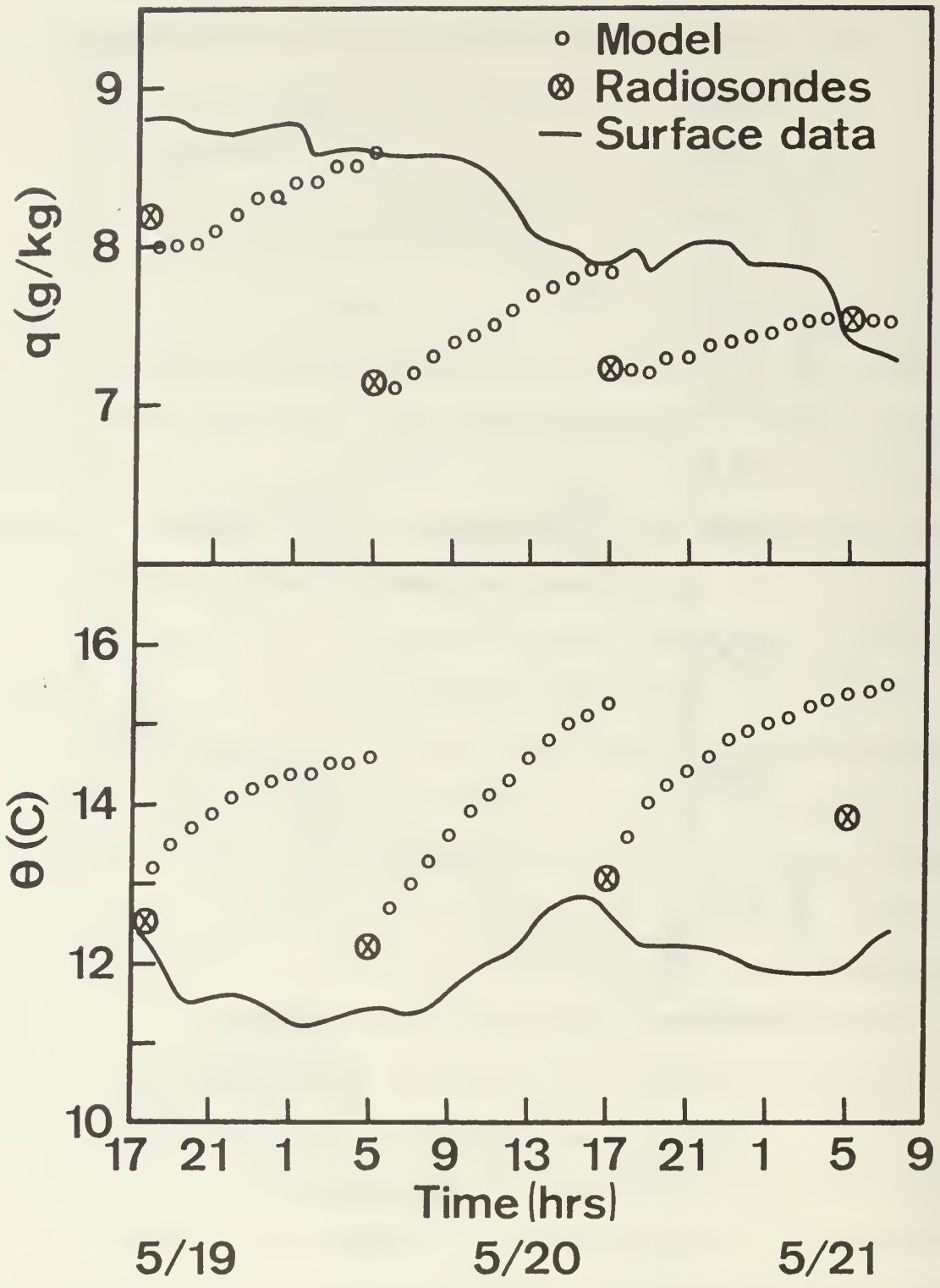

Fig. 11 Temporal evolution of the well mixed meteorological variables θ and q. The surface data were measured on the R/V ACANIA

Table IV

A comparison of Deardorff (1976), W_e, Stage and Businger (1981), W_e', entrainment rates for the initial conditions at each of the 12-hour analysis periods.

Date	Time	h(m)	Z_c(m)	Z_c/h	W_e(cm/s)	W_e'(cm/s)
5/19	1700	310	10	0.03	0.86	0.86
5/20	0500	380	270	0.71	0.84	0.42
5/20	1700	520	340	0.65	1.43	0.29

One final point to consider: the evolution shown in Fig. 9 is calculated at $S = S_o = 0.8$. Thus, applications requiring the ambient spectra including the humidity influence (for example, optical extinction) are subject to additional uncertainty due to erroneous model predictions of S (Fig. 12) and therefore g(S). This is particularly critical if $S > 0.9$.

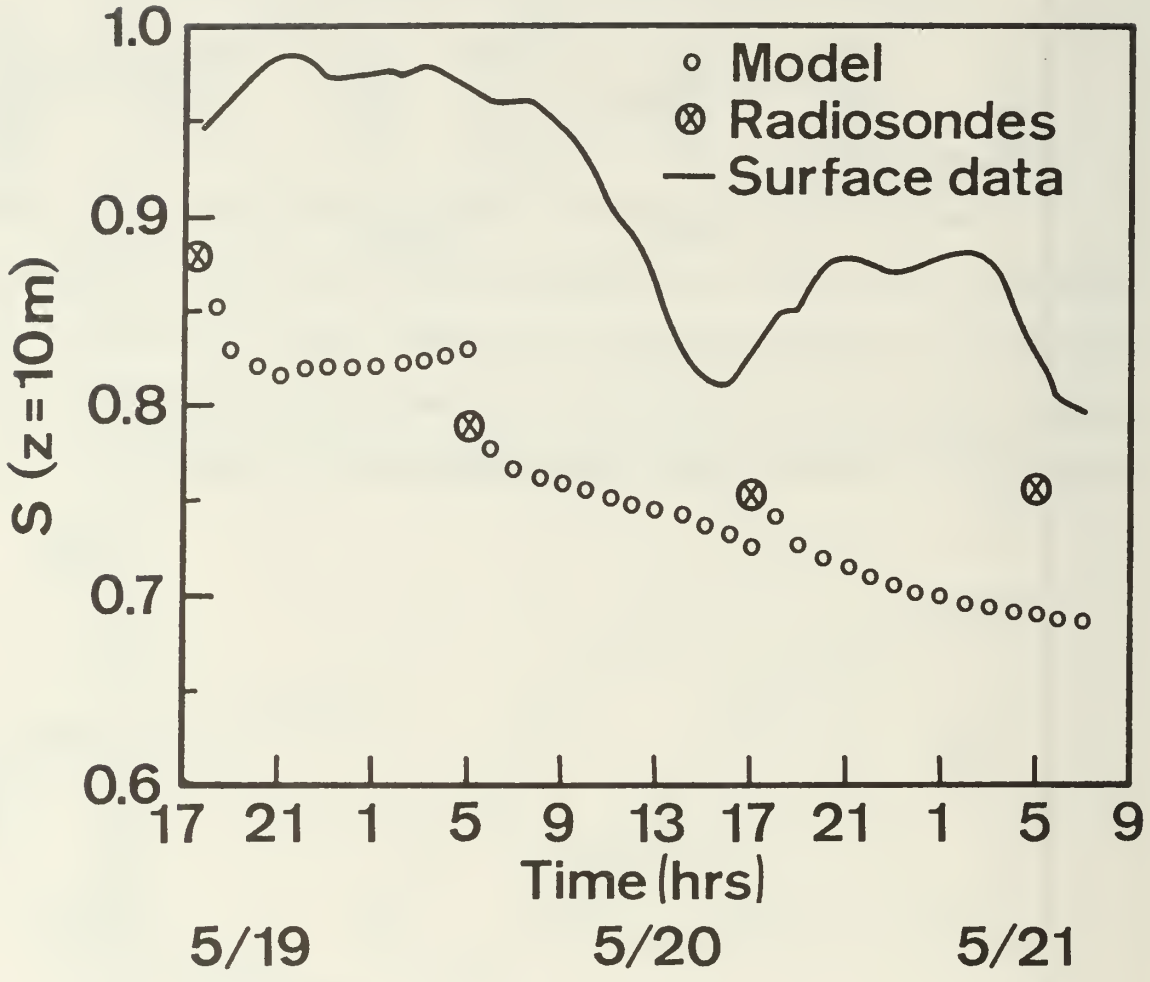

Fig. 12 Similar to Figure 11 but for the ambient saturation ratio S at Z = 10 m

8. Conclusions

The application of modern mixed layer physics to the structure and evolutions of atmospheric aerosols in the marine regime represents a philosophical quantum jump over the primarily empirical formulations of the WMK type. This was accomplished by partitioning the aerosol spectrum into continental and locally generated components and by writing the equations in terms of aerosol spectral densities transformed to a predetermined, fixed reference relative humidity. Besides the wind speed and relative humidity, the new formulation requires knowledge or specification of the entrainment rate, the mixed layer height and the sea-surface production rate of droplets. If dynamic effects are ignored, the model can predict an equilibrium aerosol spectrum (Eqn 15) roughly equivalent to that of the WMK model.

The aerosol dynamic model was tested against a marine data set in two ways. In Section 6, Eqn 13a was evaluated under optimum computational circumstances using measurements of the relevant variables wherever possible. In Section 7, a more realistic test was performed where a full mixed layer dynamic model evolution was used to simulate an actual field application of the aerosol model. In both cases the aerosol mixed layer model performed reasonably well but it did not convincingly outperform the much simpler WMK model. The errors in prediction of the aerosol spectrum and the ambient humidity represent about a factor-of-three uncertainty in the aerosol optical extinction coefficient.

Although the mixed layer model was only a modest improvement over the WMK model, it holds considerable potential for improvement. The inclusion of advective effects and improvements in the entrainment rate and aerosol surface production flux should be pursued. Another factor to consider is the nature of the aerosol production used here. The flux data given in

Table III are actually the net surface flux values which represent the droplet production minus losses due to turbulent deposition under average conditions. A modification of Table III to represent the true production and the inclusion of the turbulent deposition velocity (Slinn and Slinn, 1980) explicitly in Eqn 13, is presently under investigation.

References

Barnhardt, E. A. and J. L. Streete, 1970: A method for predicting atmospheric aerosol scattering coefficients in the infrared, Appl. Opt., 9, 1337-1344.

Blanchard, D. C. and A. H. Woodcock, 1980: The production, concentration and vertical distribution of the sea-salt aerosol. Annals N.Y Acad. Sci., 338, 330-347.

Chaen, M., 1973: Studies on production of sea-salt particles on the sea surface, Mem. Fac. Fish. Kagoshima Univ., 22, 49-105.

Davidson, K. L., G. E. Schacher, C. W. Fairall, P. Boyle and D. Brower, 1982: Marine atmospheric boundary layer modeling for tactical use, Technical report NPS 63-82-001.

Deardorff, J. W., 1976: On the entrainment rate of a stratocumulus topped mixed layer, Quart. J. Roy. Met. Soc., 102, 563-582.

Deardorff, J. W., 1978: Progress in understanding entrainment at the top of a mixed layer. Proc. Workshop on the Planetary Boundary Layer, AMS, Boston.

Fairall, C. W., K. L. Davidson and G. E. Schacher, 1981: A review and evaluation of integrated atmospheric boundary-layer models for maritime applications, Technical Report NPS 63-81-004.

Fairall, C. W., K. L. Davidson and G. E. Schacher, 1982: An analysis of the surface production of sea-salt aerosols, Technical report, NPS 63-82- .

Fitzgerald, J. W., 1975: Approximation formulas for the equilibrium size of an aerosol particle as a function of its dry size and composition and the relative humidity. J. Appl. Meteor., 14, 1044-1049.

Hughes, H. G., 1980: Aerosol extinction coefficient variations with altitude at 3.75 m in a coastal marine environment, J. Appl. Meteor., 19, 803-808.

Johnson, R. W. and W. S. Hering, 1981: Measurements of the optical atmospheric quantities in Europe and their application to modelling visible spectrum contract transmittance, Proc. 29th AGARD Symposium on EM propagation, Monterey, CA.

Lilly, D. K., 1968: Models of cloud-topped mixed layers under a strong inversion, Quart. J. R. Met. Soc., 94, 292-309.

Rosenthal, J., T. Battalino and V. R. Noonkester, 1979: Marine/continental history of aerosols at San Nicolas Island during CEWCOM-78 and OSP III, Pacific Missile Test Center, Tech. Report TP-79-33, Point Mugu, CA.

Slinn, S. A. and W.G.N. Slinn, 1980: Predictions for particle deposition on natural waters, Atmos. Environ., 14, 1013-1016.

Stage, S. A. and J. A. Businger, 1981: A model for entrainment into a cloud-topped marine boundary layer, J. Atmos. Sci., 38, Part I: Model description and application to a cold-air outbreak episode, 2213-2229. Part II: Discussion of model behavior and comparison with other models, 2230-2242.

Toba, Y., 1965: On the giant sea-salt particles in the atmosphere, II. Theory of the vertical distribution in the 10 m layer over the ocean, Tellus, 17, 365-382.

Wells, W. C., G. Gal and M. W. Munn, 1977: Aerosol distributions in maritime air and predicted scattering coefficients in the infrared, Appl. Opt., 16, 654-659.

Wu, J., 1979: Spray in the atmospheric surface layer: review and analysis of laboratory and oceanic results, J. Geophys. Res., 84, 1693-1704.

DISTRIBUTION LIST

		No. of Copies
1.	Defense Technical Information Center Cameron Station Alexandria, Virginia 22314	2
2.	Library, Code 0142 Naval Postgraduate School Monterey, California 93940	2
3.	Dean of Research, Code 012 Naval Postgraduate School Monterey, California 93940	1
4.	Professor J. Dyer, Code 61Dy Naval Postgraduate School Monterey, California 93940	1
5.	Professor R. J. Renard, Code 63Rd Naval Postgraduate School Monterey, California 93940	1
6.	Professor C.N.K. Mooers, Code 68Mr Naval Postgraduate School Monterey, California 93940	1
7.	Professor K. L. Davidson, Code 63Ds Naval Postgraduate School Monterey, California 93940	10
8.	Professor G. E. Schacher, Code 61Sq Naval Postgraduate School Monterey, California 93940	10
9.	Assoc Prof R. W. Garwood, Code 68Gd Naval Postgraduate School Monterey, California 93940	1
10.	Dr. C. W. Fairall BDM Corporation 1340 Munras Street Monterey, California 93940	10
11.	Mr. Don Spiel BDM Corporation 1340 Munras Street Monterey, California 93940	2
12.	Dr. A. Weinstein Director of Research Naval Environmental Prediction Research Facility Monterey, California 93940	1

13. CAPT K. Van Sickle 1
Naval Environmental Prediction Research Facility
Monterey, California 93940

14. Dr. A. Goroch 1
Naval Environmental Prediction Research Facility
Monterey, California 93940

15. Dr. Paul Twitchell, Code 370C 1
Naval Air Systems Command
Washington, DC 20360

16. Dr. Alex Shlanta, Code 3173 1
Naval Weapons Center
China Lake, California 93555

17. Dr. Barry Katz, Code R42 1
Naval Surface Weapons Center
White Oak Laboratory
Silver Spring, Maryland 20362

18. Dr. J. H. Richter, Code 532 1
Naval Ocean Systems Center
San Diego, California 92152

19. Dr. Lothar Ruhnke, Code 8320 1
Naval Research Laboratory
Washington, D.C. 20375

20. Mr. Herb Hitney, Code 532 1
Naval Ocean Systems Center
San Diego, California 92152

21. Mr. Herb Hughes, Code 532 1
Naval Ocean Systems Center
San Diego, California 92152

22. Mr. Stuart Gatham, Code 8320 1
Naval Research Laboratory
Washington, DC 20375

23. Commander, PMS-405 1
Naval Sea Systems Command
Washington, DC 20360

24. Dr. Steven Burke 1
Naval Environmental Prediction Research Facility
Monterey, California 93940

25. Mr. Sam Brand 1
Naval Environmental Prediction Research Facility
Monterey, California 93940

26. Mr. Paul Banas, Code 9220 1
Naval Oceanographic Office
NSTL Station, Mississippi 39522

27. Dr. Paul Moersdorf, Code 9220 1
Naval Oceanographic Office
NSTL Station, Mississippi 39522

28. LT Mark Schultz 1
Naval Environmental Prediction Research Facility
Monterey, California 93940

29. Mr. Ted Zuba, Code AIR-370 1
Naval Air Systems Command
Washington, DC 20360

30. Mr. Jay Rosenthal 1
Geophysics Division
Pacific Missile Range
Point Mugu, California 93042

31. Dr. Michael J. Kraus 1
AFGL/LYS
Hanscom AFB, Massachusettes 01731

32. MAJ Bob Wright 1
AWS/DOOE
Scott AFB, Illinois 62225

33. MAJ Ed Kolczynski 1
AWS/SYX
Scott AFB, Illinois 62225

34. Joel S. Davis 1
Defense Sciences Division
Science Applications, Inc.
1010 Woodman Drive, Suite 200
Dayton, Ohio 45432

35. Mr. L. Biberman 1
Institute for Defense Analysis
400 Army Navy Drive
Arlington, Virginia 22202

36. Dr. Richard Gomez 1
DELAS-EO-MO
Atmospheric Sciences Laboratory
White Sands, New Mexico 88002

37. Dr. R. Fenn 1
Air Force Geophysics Laboratory
Hanscom AFB, Massachusetts 02173

38. Mr. Glen Spaulding, MAT 72 1
Naval Material Command
Washington, DC 20362

39. CDR Thomas Callaham, Code N341 1
Naval Oceanography Command
NSTL Station, Mississippi 39529

40. CAPT Ronald Hughes, Commander 1
Naval Oceanography Command
NSTL Station, Mississippi 39529

41. Chief of Naval Operations, OP-952 1
ATTN: CAPT E. Young
Navy Department
Washington, DC 20350

42. Dr. Lowell Wilkens 1
Naval Weapons Center
China Lake, California 93553

43. Dr. Ed Monahan 1
Department of Oceanography
University College
Galway, IRELAND

44. Mr. Walter Martin, Code 470 1
Office of Naval Research
800 N. Quincy Street, Rm 307
Arlington, Virginia 22217

45. Dr. Gloria Patton 1
Office of Naval Research
1030 E. Green Street
Pasadena, California 91106

46. Mr. Jim Hughes, Code 470 1
Office of Naval Research
800 N. Quincy Street
Arlington, Virginia 22217

47. Dr. Warren Denner 1
Science Applications, Inc.
2999 Monterey-Salinas Hwy
Monterey, California 93940

48. Mr. George Hanssen 1
Science Applications, Inc.
P.O. Box 1303
1710 Goodrich Drive
McLean, Virginia 22102

49. Dr. Lou Goodman, Code 481 1
Office of Naval Research
Physical Oceanography
NSTL Station, Mississippi 39529

50. CDR S. G. Colgan, Code 420B 1
Office of Naval Research
800 N. Quincy Street
Arlington, Virginia 22217

51. Dr. John A. Cooney 1
Dept of Physics and Atmospheric Science
Drexel University
Philadelphia, Pennsylvania 19104

52. Mr. Thomas Rappolt 1
Energy Resources Company, Inc.
3344 N. Torrey Pines Court
La Jolla, California 92037

53. MAJ Gary G. Worley 1
Air Force Engineering and Services Center
Tyndall AFB, Florida 32403

U202242

DUDLEY KNOX LIBRARY - RESEARCH REPORTS
5 6853 01067972 3